

INITIAL ELECTRON BERNSTEIN WAVE EMISSION MEASUREMENTS ON THE TJ-II STELLARATOR

J. B. O. CAUGHMAN* *Oak Ridge National Laboratory, Oak Ridge, Tennessee*

Á. FERNÁNDEZ, Á. CAPPÀ, F. CASTEJÓN, and J. M. GARCIA-REGAÑA
Laboratorio Nacional de Fusión, EURATOM-CIEMAT, Madrid, Spain

D. A. RASMUSSEN and J. B. WILGEN *Oak Ridge National Laboratory, Oak Ridge, Tennessee*

Received February 20, 2009

Accepted for Publication June 16, 2009

Thermal electron emission at 28 GHz has been measured on the TJ-II stellarator. The emission from neutral beam-heated overdense plasmas, where the plasma density is greater than the ordinary-mode (O-mode) cutoff density, is consistent with electron thermal emission from mode-converted electron Bernstein waves (EBWs) via the Bernstein wave to extraordinary mode to ordinary mode scenario (B-X-O). Emission from underdense plasmas without neutral beam injection is consistent with the measurement of oblique electron cyclotron emission. Elec-

tron Bernstein wave emission measurements are being made to determine the optimum launch angle for planned EBW heating experiments and also to provide an indication of electron temperature evolution in overdense plasmas on TJ-II.

KEYWORDS: *electron Bernstein wave, microwave emission, TJ-II stellarator*

Note: Some figures in this paper are in color only in the electronic version.

I. INTRODUCTION

The heating of high-beta plasmas is an important issue because the high electron density precludes the use of electron cyclotron heating (ECH). Plasma heating via the electron Bernstein wave (EBW) is an attractive heating method because there is no density cutoff for the wave propagation. EBWs can be formed in the plasma either by conversion from the X-mode to the Bernstein-mode (X-B) or by conversion from the O-mode to the X-mode and then to the Bernstein mode (O-X-B). Theoretical calculations have shown that the most suitable approach for launching EBWs in the TJ-II stellarator is via O-X-B mode conversion, which is estimated to have good heating efficiency (>90%) for central densities above $1.2 \times 10^{19} \text{ m}^{-3}$ (Refs. 1 and 2). The TJ-II heliac ($l = 1$, $m = 4$) is a medium-sized stellarator operating at CIEMAT in Madrid with a major radius of 1.5 m, a minor radius of 0.2 m, and a magnetic field strength of ~ 1 T (Ref. 3). The plasmas are created and heated by ECH via two 300-kW gyrotrons at second-harmonic X-mode

(53.2 GHz), with additional heating provided by two neutral beam injectors. Once the cutoff density is reached, however, no more ECH power is absorbed in the central plasma; thus, other heating options are needed. Current plans for EBW heating are to use a 28-GHz system, which will deliver 300 kW through a section of corrugated waveguide.⁴ The microwave heating beam will be focused and directed into the plasma by a steering mirror located inside the vacuum vessel. In the O-X-B scenario, efficient mode conversion and heating are highly dependent on the orientation of the launched wave with respect to the external magnetic field.⁵ It is important, therefore, to find the optimum experimental orientation angle that maximizes the mode conversion efficiency.

Prior to the heating experiments, the measurement of the thermal EBW emission from the plasma is being used to determine the optimum launch angle and the mode conversion efficiency. Similar experiments have been done on several machines.⁶⁻⁸ Using reciprocity, the optimum launch angle of the heating wave can be determined by finding the viewing angle that maximizes the thermal emission intensity in overdense plasmas.^{9,10} In these plasmas, the EBWs are a good blackbody emitter because of

*E-mail: caughmanjb@ornl.gov

the high optical thickness.¹¹ The measured emission is dependent on both the orientation of the magnetic field angle with respect to the viewing antenna (horn) and the polarization of the wave. Emission-dependent orientation can be checked by using a movable mirror in the vacuum chamber for changing the viewing angle and also for further focusing of the viewing beam. Polarization is not determined directly, but two orthogonally polarized components of the microwave emission from the plasma are measured with a dual-polarized quad-ridged horn. The horn is oriented such that one channel measures emission parallel to the magnetic field while the other channel measures emission perpendicular to the field. The ratio of the channels can be used to check consistency with the expected elliptical polarization.

II. DIAGNOSTIC DESIGN

The microwave emission measurement diagnostic is shown in Fig. 1. Details of the design can be found in Ref. 12, but a brief description will be given here. The system consists of a remotely movable focusing mirror (170×190 mm) located inside the vacuum chamber, a reflector (flat mirror) attached to a section of corrugated waveguide, a glass focusing lens, and a Flann model DP241-AB quad-ridged dual-polarized microwave horn. The focusing lens and the horn are located outside the vacuum chamber. The microwave emission from the plasma (at 28 GHz) is reflected from the focusing mirror into the detection waveguide via the flat mirror. The emission is then focused into the microwave horn via a glass mirror (BK-7), which has an optical focal length of 250 mm. The ridges of the horn are aligned with the magnetic field such that one channel measures the emission with the electric field vector parallel to the magnetic field, while the other channel measures the emission with

the electric field vector perpendicular to the magnetic field. The movable focusing mirror is used to spatially scan the plasma for the emission measurement experiments and also to steer the microwave beam for the heating experiments,⁴ although not at the same time.

The emission measurement system is mounted on a bellows so that it can be extracted upward so as not to interfere during the heating experiments. A gate valve, located between the emission waveguide and the microwave horn, is closed during the heating experiments to protect the sensitive electronics used for the emission measurements. The microwave signals from the horn are coupled via low-loss coaxial cable to a two-channel radiometer. Bandpass filters ($28 \text{ GHz} \pm 0.5 \text{ GHz}$) are used on the radiometer inputs such that only the emission near 28 GHz is measured. The radiometer is a heterodyne design with a fixed frequency local oscillator (28.8 GHz) feeding two mixer preamplifiers. The intermediate frequency output signal of each mixer preamplifier flows through a bandpass filter ($800 \text{ MHz} \pm 50 \text{ MHz}$) and is then amplified with a detector log video amplifier (bandwidth $>20 \text{ MHz}$).

The entire system, including waveguide, gate valve, and lens, was calibrated using a chopper wheel arrangement that alternated between microwave absorbers at room temperature and liquid nitrogen. The radiometer signals represent the effective blackbody radiation temperature. The output signals were acquired at a rate of 1 MHz by the TJ-II data acquisition system. Because of the inherent fluctuations in thermal noise emission and the high video bandwidth,¹³ the fluctuation level of the raw data was $\pm 60\%$ of the signal level. Therefore, a 50-point smoothing factor was used for all the EBW emission (EBE) radiometer data shown below. This smoothing factor resulted in a fluctuation level of roughly $\pm 5\%$ of the acquired signal level, which is more consistent with the other machine data presented [e.g., central electron

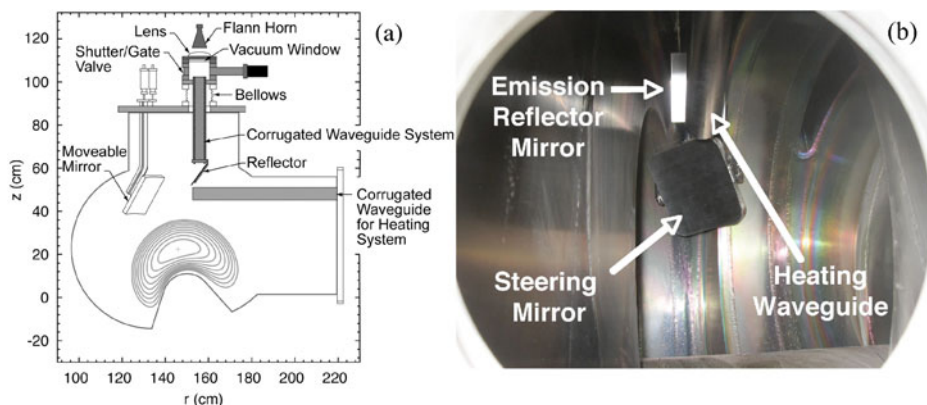


Fig. 1. A schematic of the EBE measurement system. (a) The same movable steering mirror is used for both the heating waveguide (on the right) and the emission waveguide (at the top), although not at the same time. (b) The installed system, as viewed from the mounting flange for the heating system corrugated waveguide.

cyclotron emission (ECE) signal, which uses a 20-kHz video bandwidth as mentioned below].

III. INITIAL EMISSION MEASUREMENT RESULTS

The plasmas in TJ-II are produced by electron cyclotron resonance heating (ECRH) from two 300-kW gyrotrons operating at 53.2 GHz. Additional heating is provided by neutral beam injectors, nominally operated at 30 kV and 400 kW (Ref. 14). Typical diagnostics for the discharges include the line density, second-harmonic X-mode ECE, soft-X-ray emission, and Thomson scattering. The ECE system is a 16-channel single-sideband heterodyne radiometer with a frequency range of 49 to 64 GHz, where each channel has a 3-dB bandwidth of 150 MHz (Ref. 15). The video bandwidth of each channel is set to 20 kHz using low-pass filters. The Thomson scattering diagnostic gives one density and temperature profile per shot. Microwave emission from the plasma at 28 GHz was measured for ECRH discharges both with and without neutral beam injection (NBI). For the initial experiments, the internal steering mirror remained fixed at the theoretical optimum angle for maximum O-X-B conversion efficiency, based on ray-tracing calculations for power absorption using the TRUBA code.²

Microwave emission at 28 GHz from an underdense plasma is consistent with the measurement of oblique O-mode ECE. Results from a typical discharge without NBI are shown in Fig. 2. For this shot (17802), the total injected ECRH power was ~ 300 kW (from one gyrotron). The 28-GHz emission radiation temperature measured approximately parallel to the magnetic field is shown in Fig. 2a, while the radiation temperature measured approximately perpendicular to the magnetic field is shown in Fig. 2b. The sum of the two channels corresponds to the total radiation temperature. The ECE signal from the center region of the plasma (54.95 GHz) is shown in Fig. 2c, and the line density is shown in Fig. 2d. The shape of the 28-GHz emission from both radiometer channels is very similar to the ECE signal. While the line density is less than the O-mode cutoff density of $9.72 \times 10^{18} \text{ m}^{-3}$ during the entire shot, it is possible that some of the emission could have come from B-X-O mode conversion if there were local areas of the plasma that were above the cutoff density. However, Thomson scattering results (discussed below) show that almost all of the plasma density profile is below the cutoff density, which would imply that the majority of the 28-GHz emission signal seems to be a measurement of oblique fundamental O-mode ECE.

Both radiometers indicate similar radiation temperatures and have fluctuation levels of $\sim 30\%$ of the average signal. Oblique O-mode emission is expected to be elliptically polarized,¹⁶ with an estimated ellipticity angle of the polarization ellipse at the plasma boundary (χ) of

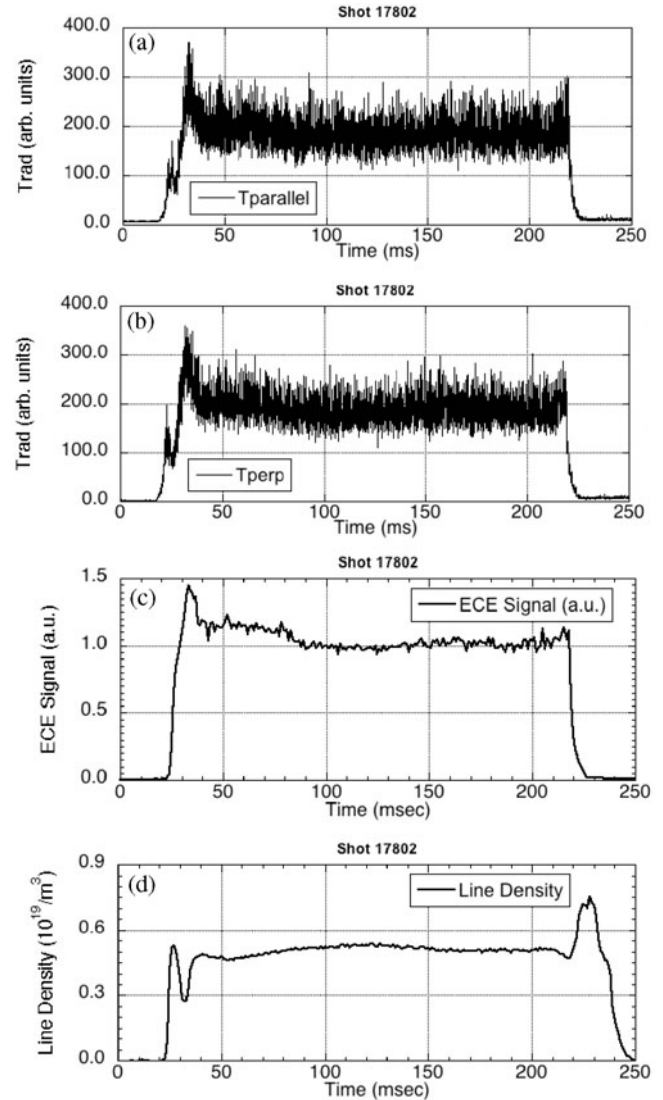


Fig. 2. Results without NBI for shot 17802. (a) EBE radiometer signal of the parallel channel, (b) EBE radiometer signal of the perpendicular channel, (c) central ECE signal, and (d) line density.

35 deg for conditions on TJ-II. The theoretical power ratio between polarization components is given by

$$\eta = \frac{P_{\parallel}}{P_{\perp}} \equiv \left(\frac{\cos \chi}{\sin \chi} \right)^2 \approx 2,$$

which is also the expected ratio between radiation temperatures. The measured ratio of the parallel to perpendicular radiation temperatures was close to unity. The fact that they were measured to be nearly equal could indicate the measurement of scattered radiation, or it could indicate that the microwave horn was not properly oriented with respect to the magnetic field. The source of

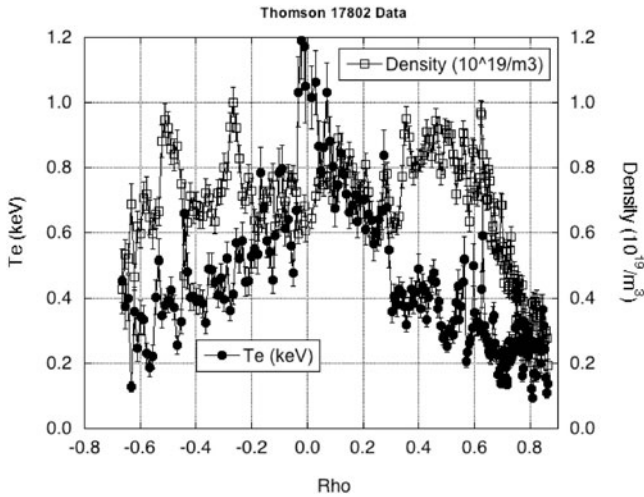


Fig. 3. Thomson scattering measurement without NBI for shot 17802. The data were taken at 189 ms.

the fluctuation is not clear at this time, but factors that could contribute to it include thermal noise emission and the high bandwidth of the video amplifier of the radiometer (>20 MHz) (Ref. 13), the choice of the smoothing

factor for data analysis, or possibly actual temperature fluctuations. Subsequent measurements using a 32-kHz low-pass filter on the radiometer video amplifier have reduced the radiation temperature fluctuation levels to approximately $\pm 12\%$ of the average signal, indicating the influence of the radiometer electronics. Future experiments will look at the source of the fluctuation in more detail.

The density and temperature profiles from the Thomson scattering diagnostic for this shot (17802) are shown in Fig. 3. The profile was measured at a time of 189 ms. The density profile shows a relatively broad distribution, while the temperature profile is peaked in the center. The total radiation temperature from the 28-GHz emission, at the time that the Thomson profile was taken, was measured to be 370 ± 80 eV. Direct comparisons between the Thomson data and the 28-GHz emission data are difficult to make for oblique ECE because the plasma is optically thin, so the plasma is not a good blackbody emitter, as confirmed by ray-tracing calculations. The results of a single nonrelativistic ray-tracing calculation are shown in Fig. 4 for the conditions of shot 17802. The ray is shown as an obliquely propagating O-mode launched from the detection horn. The result shows that the ray propagates through the plasma, and the power absorption is very low ($\sim 3\%$). Integration of

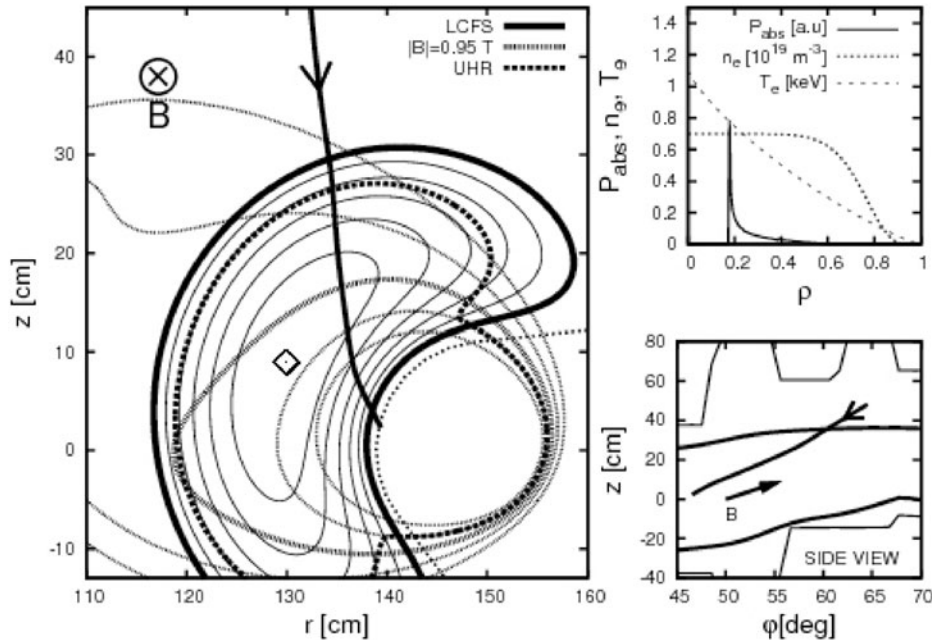


Fig. 4. Single nonrelativistic ray-tracing calculation of an obliquely propagating O-mode as if it were launched from the detection antenna. The projection of the ray trajectory in the toroidal TJ-II plane where maximum absorption occurs is represented in the left panel. Bottom right panel presents a side view of the trajectory in the plasma. Power absorption and plasma profiles are represented in the top right panel. Power absorption (in arbitrary units) is very low ($\sim 3\%$). The density and temperature profiles used in the calculation were obtained by fitting the Thomson scattering data presented in Fig. 3 [$n_e = 0.7 \times (1 - \psi^4)^7$ and $T_e = 1.1 \times (1 - \psi^{0.4})^{1.2}$, where ψ is the normalized magnetic flux].

the absorption coefficient along the beam path gives a calculated optical thickness of only $\sim 2.8 \times 10^{-2}$.

Microwave emission at 28 GHz from an overdense plasma is consistent with the measurement of mode-converted EBWs. Results from a typical discharge with

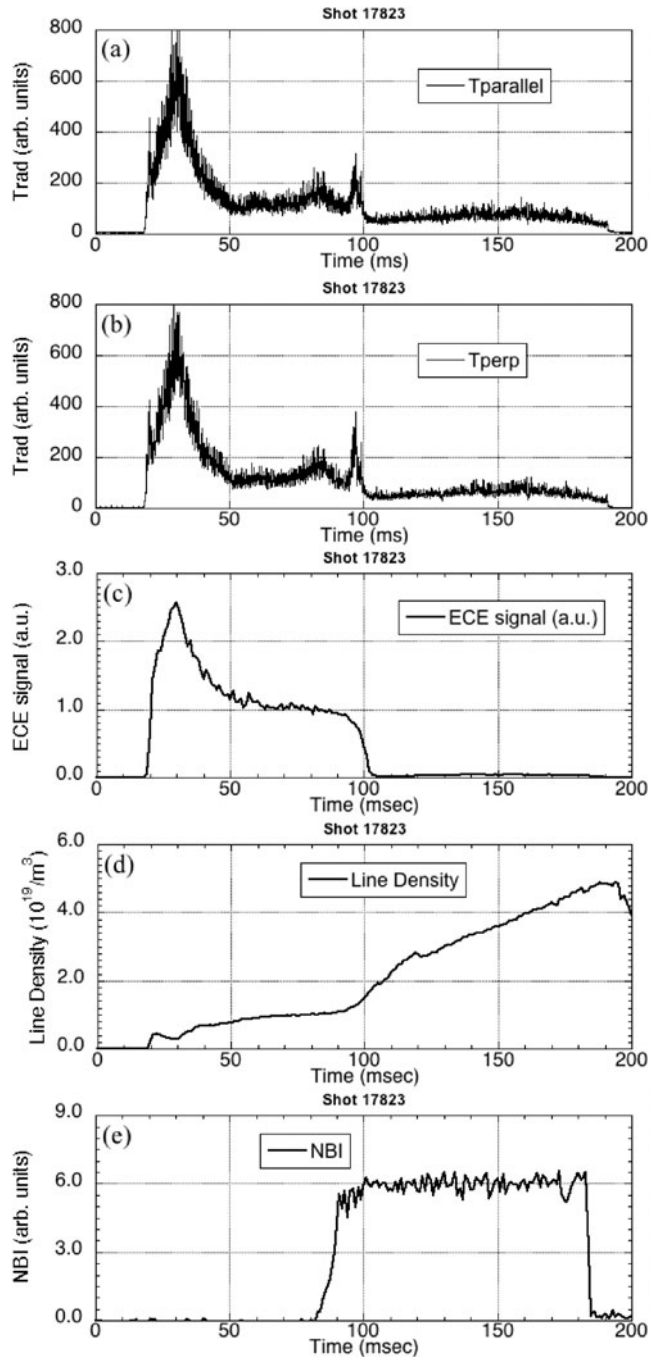


Fig. 5. Results with NBI for shot 17823. (a) EBE radiometer signal of the parallel channel, (b) EBE radiometer signal of the perpendicular channel, (c) central ECE signal, (d) line density, and (e) neutral beam grid voltage.

NBI are shown in Fig. 5. For this shot (17823), the total injected ECH power was ~ 600 kW. The 28-GHz radiation temperature is shown in Fig. 5a for parallel emission and in Fig. 5b for perpendicular emission. Initially, both channels follow the general shape of the ECE signal shown in Fig. 5c, with a temperature peak at the initial formation of the plasma, followed by a gradual decline. The line density, shown in Fig. 5d, declines slightly at the beginning of the pulse and then starts to gradually increase. NBI is initiated near 90 ms, as shown in Fig. 5e. Shortly after NBI starts, the line density increases significantly. By 100 ms, the line density is beyond cutoff for the second-harmonic X-mode, and the ECE signal drops dramatically. As with shot 17802, the 28-GHz emission at the beginning of the pulse is consistent with the measurement of oblique ECE at least until ~ 70 ms, since the line density is below the O-mode cutoff density. There is a spike in the emission near the time when NBI starts. The reason for this spike, which may be due to emission from nonthermal electrons or possibly caused by refraction of the waves during the transition to overdense conditions, is not understood at this time and will require further study. While the plasma is clearly in an overdense

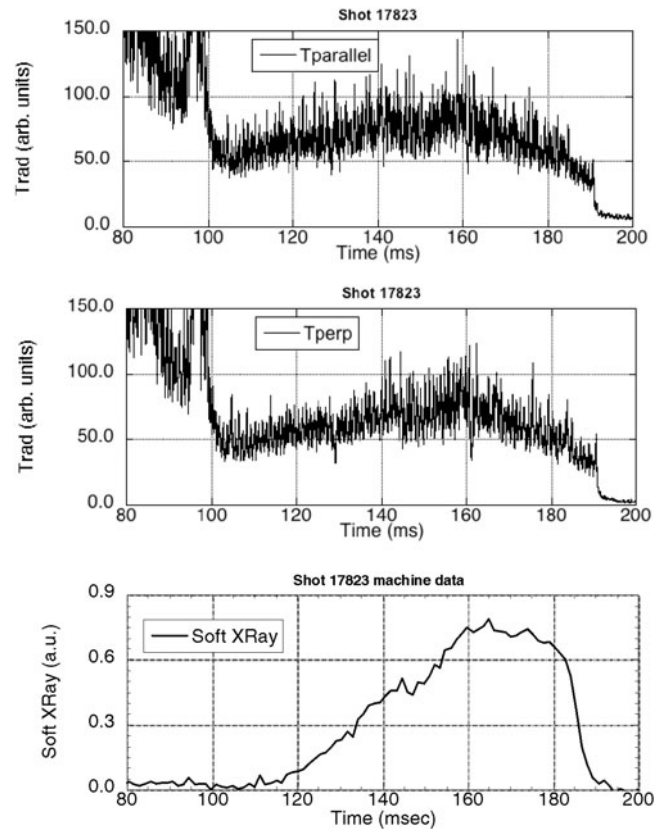


Fig. 6. Results with NBI for shot 17823 during overdense conditions. (a) EBE radiometer signal of the parallel channel, (b) EBE radiometer signal of the perpendicular channel, and (c) soft-X-ray data.

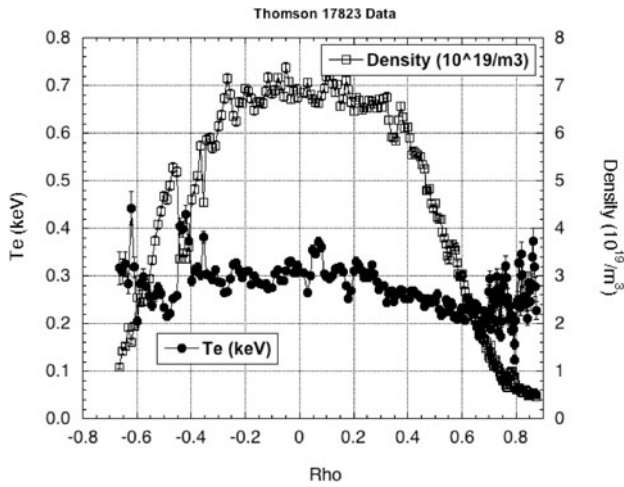


Fig. 7. Thomson scattering measurement with NBI for shot 17823. The data were taken at 155 ms.

condition beyond 100 ms, there is still significant emission at 28 GHz, which is presumably from electron thermal emission via B-X-O mode conversion. The 28-GHz emission during overdense conditions is shown in more

detail in Fig. 6, where the parallel emission is shown in Fig. 6a and the perpendicular emission is shown in Fig. 6b. The radiation temperature increases gradually until it peaks near 160 ms, which is consistent with the shape of the soft-X-ray signal shown in Fig. 6c. The similarity with the time evolution of the soft-X-ray signal is another indication that the 28-GHz emission in overdense conditions corresponds to EBE. The ratio of the parallel to perpendicular temperatures during the discharge is initially close to 1.0 but changes to a ratio of 1.1 when the plasma goes overdense, which is still below the predicted value of 2.0.

The plasma density and electron temperature profiles from Thomson scattering for this shot (17823) are shown in Fig. 7. The data were taken at 155 ms. The density profile is peaked in the center, and the temperature profile is fairly flat. The electron temperature varies from 260 to 360 eV across most of the profile, while the total EBE radiation temperature at this point in time is estimated to be 160 ± 40 eV. Ray-tracing calculations show that power absorption should be good for these overdense plasma conditions. The results of a single non-relativistic ray-tracing calculation are shown in Fig. 8 for the conditions of shot 17823. The ray is shown as an obliquely propagating O-mode launched from the

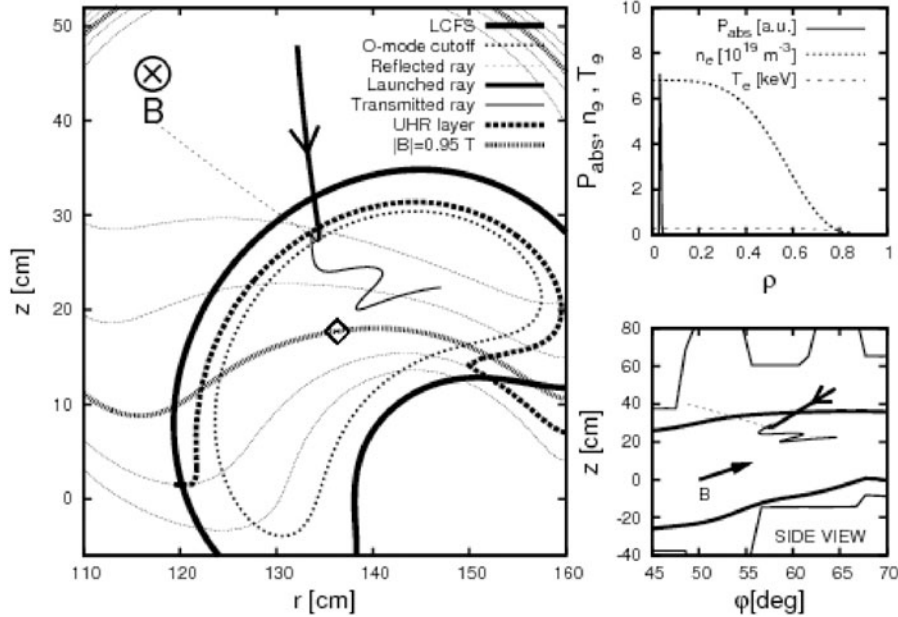


Fig. 8. Same launching configuration as in Fig. 4 but for the density and temperature profiles obtained in the NBI phase of shot 17823. The O-X-B projection of the ray trajectory in the toroidal TJ-II plane is represented in the left panel. Bottom right panel presents a side view of the trajectory in the plasma. Power absorption and plasma profiles are represented in the top right panel. The O-mode cutoff for this density profile is located around $\rho = 0.7$. Power deposition is very peaked near the plasma center. The density and temperature profiles used in the calculation were obtained by fitting the Thomson scattering data presented in Fig. 7 [$n_e = 6.8 \times (1 - \psi^2)^7$ and $T_e = 0.27 \times (1 - \psi^7)^{10}$, where ψ is the normalized magnetic flux]. For this density profile (overdense plasma), O-X conversion takes place with 99% efficiency for this single ray calculation, and full central absorption of the EBW occurs.

detection horn. The O-mode wave converts to an X-mode at the O-mode cutoff layer ($\rho = 0.7$) and is then converted to the Bernstein mode at the upper hybrid resonant layer. The calculation shows that the power absorption is very high, with O-X mode conversion occurring with 99% efficiency and then full absorption of the EBW. The power absorption is very peaked near the plasma center (near $\rho = 0$). While it is tempting to get an initial estimate of the B-X-O mode conversion efficiency by comparing the ratio of the radiation temperature to the electron temperature, such an estimate is premature at this time. Further modeling of the expected emission is needed for these plasma conditions to better understand the origin of the emission, the expected polarization, and the effect of the beam shape on the emission results. Calculations of wave absorption show that the conversion efficiency can vary from 0.52 to 0.86 and is dependent on the spot size of the microwave beam and the curvature of the plasma relative to the beam.¹⁷ These dependences need to be taken into account with respect to interpreting the microwave emission.

IV. SUMMARY AND FUTURE WORK

Initial measurements of 28-GHz emission from the TJ-II plasma have been made. The emission was measured with a dual-polarized microwave horn that is oriented such that it measures emission both parallel and perpendicular to the external magnetic field. When the plasma is operated below the O-mode cutoff density, the time evolution of the 28-GHz emission is consistent with measuring oblique fundamental O-mode ECE. When the plasma is in overdense conditions during NBI, the emission is consistent with the measurement of B-X-O mode conversion, and the time evolution of the emission is similar to that seen in the soft-X-ray emission. The polarization of the emission is close to 1.0 during underdense conditions and increases to 1.1 during overdense conditions, which is considerably lower than the predicted value of 2.0. A factor that contributes to this difference includes the orientation of the radiometer with respect to the magnetic field, which will be the subject of future experiments in both low- and high-density plasmas. Measurement results will be further compared to ray-tracing calculations to help us understand the origin of the detected emission. Another major experimental effort will be to measure the EBE as a function of orientation angle of the internal steering mirror. The goal of these experiments will be to find the mirror orientation for maximum emission, which will help to determine the optimum launch angle for efficient EBW heating.

ACKNOWLEDGMENTS

The authors would like to acknowledge helpful discussions with E. de la Luna of CIEMAT, currently working on

JET, and G. Taylor of the Princeton Plasma Physics Laboratory. Oak Ridge National Laboratory is managed by UT-Battelle, LLC, for the U.S. Department of Energy under contract DE-AC05-00OR22725. A part of this work is performed under support of Spanish "Subdirección General de Proyectos de Investigación, Ministerio de Educación y Ciencia" with reference ENE2004-06957.

REFERENCES

1. F. CASTEJÓN et al., "Weakly Relativistic and Nonrelativistic Estimates of EBW Heating in the TJ-II Stellarator," *Fusion Sci. Technol.*, **52**, 230 (2007).
2. F. CASTEJÓN et al., *Nucl. Fusion*, **48**, 075011 (2008).
3. C. ALEJALDRE et al., "TJ-II Project: A Flexible Helical Stellarator," *Fusion Technol.*, **17**, 131 (1990).
4. A. FERNÁNDEZ et al., *Fusion Eng. Design*, **74**, 325 (2005).
5. E. MJØLHUS et al., *J. Plasma Phys.*, **31**, 7 (1984).
6. G. TAYLOR et al., *Phys. Plasmas*, **12**, 052511 (2005).
7. J. PREINHAELTER et al., *Rev. Sci. Instrum.*, **74**, 1437 (2003).
8. H. P. LAQUA et al., *Phys. Rev. Lett.*, **81**, 2060 (1998).
9. A. D. PILIYA and A. POPOV, *Plasma Phys. Control. Fusion*, **44**, 467 (2002).
10. A. K. RAM and A. BERS, *Nucl. Fusion*, **43**, 1305 (2003).
11. P. C. EFTHIMION et al., *Rev. Sci. Instrum.*, **70**, 1018 (1999).
12. J. B. O. CAUGHMAN et al., "The Electron Bernstein Wave Emission Viewing System for the TJ-II Stellarator," *Proc. 14th Joint Workshop ECE and ECRH*, Santorini Island, Greece, May 9–16, 2006, p. 243, A. LAXAROS, Ed., Heliotopos Conferences (2006).
13. H. J. HARTFUSS et al., *Plasma Phys. Control. Fusion*, **39**, 1693 (1997).
14. M. LINIERS et al., "Recent Results with NBI Plasma in TJ-II Stellarator," *Proc. 15th Int. Stellarator Workshop*, Madrid, Spain, October 3–7, 2005.
15. E. DE LA LUNA et al., *Rev. Sci. Instrum.*, **72**, 379 (2001).
16. F. VOLPE et al., *Rev. Sci. Instrum.*, **74**, 1409 (2003).
17. A. KÖHN et al., *Plasma Phys. Control. Fusion*, **50**, 085018 (2008).